PHYSICAL REVIEW D **82,** 034003 (2010)

$\eta - \eta'$-glueball mixing

Simon Kiesewetter and Vicente Vento

Departament de Física Teòrica and Institut de Física Corpuscular, Universitat de València-CSIC, E-46100 Burjassot (Valencia), Spain

(Received 13 April 2010; published 5 August 2010)

We have revisited glueball mixing with the pseudoscalar mesons in the MIT bag model scheme. The calculation has been performed in the spherical cavity approximation to the bag using two different fermion propagators, the cavity and the free propagators. We obtain probabilities of mixing for the η at the level of 0.006%–2.0%, while for the η' one at the level of 0.6%–40%, depending on the choice of bag radius and, therefore, of the strong coupling constant. Our results differ from previous calculations. The origin of our difference stems from the treatment of the time integrations. The comparison of our calculation with experimental data, which is consistent with small $\eta - \eta' - G$ mixing, implies that the pseudoscalar glueball is small, $R \sim 0.5$–0.6 fm and has a large mass, $M_G \sim 2000$–2500 MeV.

DOI: 10.1103/PhysRevD.82.034003 PACS numbers: 12.39.Mk, 12.39.Ba, 14.40.−n, 14.65.Bt

I. INTRODUCTION

Quantum chromodynamics (QCD) is the theory of the hadronic interactions. It is an elegant theory whose full nonperturbative solution has escaped our knowledge since its formulation more than 30 years ago [1]. The theory is asymptotically free [2,3] and confining [4]. A particularly good test of our understanding of the nonperturbative aspects of QCD is to study particles where the gauge field plays an important dynamical role. For this reason, the glueball spectrum has attracted much attention [5].

From the phenomenological point of view it has become clear by now that it is difficult to single out which states of the hadronic spectrum are glueballs because we lack the necessary knowledge to determine their decay properties. Moreover, the strong expected mixing between glueballs and quark states leads to a broadening of the possible glueball states which does not simplify their isolation. A comprehensive review on the experimental status of glueballs has recently appeared [6]. For the purposes of this paper we accept the existence of at least one pseudoscalar glueball state, although its existence has been a matter of debate since the Mark II experiment proposed glueball candidates [7]. Note that the pseudoscalar sector is a complex one. On the one hand, it accommodates the Goldstone nature of the pseudoscalar multiplet, on the other, not totally unrelated, we encounter the singlet-octet mixing, which is traditionally associated with the resolution of $U(1)$ anomaly. In constituent models, the ideal mixing ($\theta_i = \tan^{-1}\sqrt{2}$) is natural, however the η and η' mixing is nonideal due to the anomaly.

Gluon self-couplings in QCD suggest the existence of glueballs, bound states of mainly gluons [8]. Investigating glueball physics requires an intimate knowledge of the confining QCD vacuum and it is well known that such properties cannot be obtained using standard perturbative techniques. To handle the nonperturbative regime of QCD, one can resort to numerical methods, known as lattice QCD. Lattice QCD needs as input the quark masses and an overall scale, conventionally given by Λ_{QCD}. Then any Green function can be evaluated by taking averages of suitable combinations of lattice fields in vacuum samples. This allows masses and matrix elements, particularly those of weak or electromagnetic currents, to be studied. However, lattice QCD faces both computational and fundamental problems in the description of glueballs [5]. A complementary way to describe glueballs, namely, the MIT bag model, implements in a dynamical way the phenomenological properties of the confining QCD vacuum and the interaction among the gluons. Historically the investigation of the glueball properties started precisely in this model [9]. Jaffe and Johnson found many glueball states with different quantum numbers lying in the mass interval 1000–2000 MeV.

The aim of the present investigation is the study of the mixing between a possible pseudoscalar glueball state and the η or η'-mesons. The calculation has been performed in the MIT bag model, a description which imposes by *fiat* some of the properties of QCD. In this model, a hadron is basically a bubble of perturbative vacuum in the midst of a nonperturbative vacuum. Inside the bubble we insert the constituents, which are described by cavity modes, and the surface of the bubble screens color from flowing into the nonperturbative world. The calculation has been performed in the so-called spherical cavity approximation, where several improvements have been incorporated, like center-of-mass corrections and the recoil correction. In this setup, the cavity is fixed to be a sphere and its radius is allowed to vary dynamically. Within this scheme we have performed two calculations of the mixing Hamiltonian. One, in which we have used the cavity propagator for the quarks. This cavity propagator is made up of a sum over all possible cavity states. Thus it incorporates, in principle, the confining property of the bag model. Another, in which we have used the free propagator which is described in terms of free modes. As it turns out, the results of both calculations are almost the same, so the

 © 2010 The American Physical Society

dominating property, at least for the problem investigated here, is asymptotic freedom.

Our investigation is presented as follows. In Sec. II we show the necessary tools to carry out the calculation. Starting from the QCD Lagrangian we use a formalism that allows one to calculate the mixing energies perturbatively by means of the appropriate Feynman diagrams. We have to introduce for this purpose the bare glueball and meson states. In Sec. II C, we discuss the quantization, which is important since the problem at hands is a multiparticle one. After discussing the role of the propagator in Sec. II C, and addressing and resolving an important physical problem that arises in bag model calculations in Sec. II D, we present and comment on the results in Sec. III and give some conclusions in Sec. IV. The actual calculations have been relegated to the appendix to ease the reading of the main text.

II. CALCULATION OF THE η-η'-GLUEBALL MIXING IN THE BAG MODEL

We next calculate the mixing energy, which corresponds to off-diagonal Hamiltonian terms in Fock space. In subsection II A, we introduce a formalism which allows the calculation of the mixing energies in a perturbative manner. In subsection II B we present the bare glueball and meson states in the bag model. Thereafter we discuss important aspects of the calculation.

A. Formalism

QCD is a non-Abelian Yang-Mills theory with a $SU(3)$ gauge symmetry regarding color charge. The Lagrangian is

$$\mathcal{L}_{\mathrm{QCD}} = \bar{\psi}(i\not{\partial} - m)\psi - \tfrac{1}{4}F^a_{\mu\nu}F^{\mu\nu}_a, \tag{1}$$

where

$$D_\mu = \partial_\mu - igA^a_\mu t^a \tag{2}$$

$$F^a_{\mu\nu} = \partial_\mu A^a_\mu - \partial_\nu A^a_\mu + gf^{abc}A^b_\mu A^c_\nu. \tag{3}$$

$t^a = \frac{1}{2}\lambda^a$ where λ^a are the Gell-Mann matrices and f^{abc} are the structure constants of the $SU(3)$ algebra. Some rearrangement yields

$$\begin{aligned}\mathcal{L}_{\mathrm{QCD}} = {} & \underbrace{\bar{\psi}(i\not{\partial} - m)\psi}_{\mathcal{L}_{0_A}} \\ & - \underbrace{\tfrac{1}{4}(\partial_\mu A^a_\nu - \partial_\nu A^a_\mu)(\partial^\mu A^\nu_a - \partial^\nu A^\mu_a)}_{\mathcal{L}_{0_B}} \\ & + \underbrace{g\bar{\psi}\gamma^\mu A^a_\mu t^a \psi}_{\mathcal{L}_1} - \underbrace{g(\partial_\mu A^a_\nu)f^{abc}A^\mu_b A^\nu_c}_{\mathcal{L}_2} \\ & - \underbrace{\tfrac{1}{4}g^2(f^{abc}A^b_\mu A^c_\nu)(f^{abc}A^\mu_b A^\nu_c)}_{\mathcal{L}_3},\end{aligned} \tag{4}$$

where we can identify the free Lagrangian of QED ($\mathcal{L}_0$) with color indices, a quark-quark-gluon vertex ($\mathcal{L}_1$), a 3-gluon vertex ($\mathcal{L}_2$) and a 4-gluon vertex ($\mathcal{L}_3$).

We use a perturbative approach inside the cavity following the scheme developed by Maxwell and Vento [10]. The glueball and meson states represent solutions of the free Lagrangian $\mathcal{L}_{0_A}$ and $\mathcal{L}_{0_B}$, respectively. The equations of motion arising from the Lagrangian of QCD are

$$(i\not{\partial} - m)\psi = g\gamma^\mu A^a_\mu t^a \psi \tag{5}$$

and

$$\begin{aligned}\partial_\mu(\partial^\mu A^\nu_a - \partial^\nu A^\mu_a) = {} & -gf^{abc}\partial_\mu(A^\mu_b A^\nu_c) - gf^{abc}A^b_\mu F^{\mu\nu}_c \\ & - g\bar{\psi}\gamma^\nu t_a \psi.\end{aligned} \tag{6}$$

Equations (5) and (6) can be understood as an inhomogenous Dirac equation and Maxwell equation, respectively. Thus, they can be solved exactly using the Feynman propagator for the Dirac and the Maxwell fields in the following way

$$\psi(x) = g\int d^4x' S_F(x,x')\gamma^\mu A^a_\mu(x')t^a\psi(x') \tag{7}$$

and

$$\begin{aligned}A^\mu_a(x) = {} & g\int d^4x' D_F(x,x')[-f^{abc}\partial_\mu(A^\mu_b(x')A^\nu_c(x')) \\ & - f^{abc}A^b_\mu(x')F^{\mu\nu}_c(x') - \bar{\psi}\gamma^\nu t_a\psi].\end{aligned} \tag{8}$$

One can now expand $\psi(x)$ and $A^\mu(x)$ in a power series of g and obtains for the first order term

$$\psi^{(1)}(x) = \psi^{(0)} + g\int d^4x' S_F(x,x')\gamma^\mu A^{(0)a}_\mu(x')t^a\psi^{(0)}(x') \tag{9}$$

$$\begin{aligned}A^{(1)\mu}_a(x) = {} & A^{(0)} + g\int d^4x' D_F(x,x') \\ & \times[-f^{abc}\partial_\mu(A^{(0)\mu}_b(x')A^{(0)\nu}_c(x')) \\ & + f^{abc}A^{(0)b}_\mu(x')F^{(0)\mu\nu}_c(x')].\end{aligned} \tag{10}$$

One can now use the expressions $\psi^{(1)}$ and $A^{(1)}$ or higher orders of ψ and A to calculate the expectation value $\langle\hat{\Gamma}\rangle$ of some observable $\hat{\Gamma}$ to various perturbative orders of g. In here we are interested in the expectation value of the quark-gluon interaction Hamiltonian $\hat{H}_I = g\bar{\psi}\gamma^\mu A^a_\mu t^a\psi$. Inserting $\psi^{(1)}$ yields

$$\begin{aligned}\langle\bar{H}_I\rangle = {} & g\int d^3x\bar{\psi}^{(1)}(x)\gamma^\mu A^{(0)}(x)^a_\mu t^a\psi^{(0)}(x) \\ & + g\int d^3x\bar{\psi}^{(0)}(x)\gamma^\mu A^{(0)}(x)^a_\mu t^a\psi^{(1)}(x)\end{aligned} \tag{11}$$

$$= 2g^2 \int d^3x \bar{\psi}(x)\gamma^\mu A(x)^a_\mu t^a \times \int d^4x' S_F(x, x')\gamma^\nu A(x')^b_\nu t^b \psi(x') \quad (12)$$

with zero order wave functions in Eq. (12). This expression corresponds to an exchange of a virtual fermion as shown in Fig. 1. Inserting different orders of ψ and A, one obtains expressions corresponding to different Feynman diagrams. Every order in ψ brings a fermion propagator, while every order in A brings a gluon propagator. For our calculation, we will restrict ourselves to the one-fermion exchange, since this is the leading-order diagram of the meson-gluon interactions. The lowest-order gluon exchange diagram, shown in Fig. 1, does not contribute, because the gluon is a spin-1 particle and therefore does not couple to the spin-0 pseudoscalar meson or glueball. Another argument to show the vanishing of this contribution has to do with color. The color structure tells us that a color singlet gluon state does not exist and since the quark and antiquark states are in a color singlet state, the diagram has to vanish.[1]

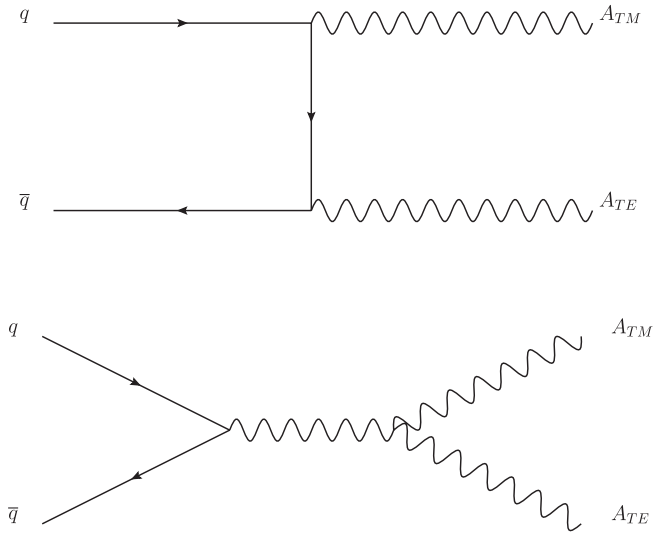

FIG. 1. Fermion exchange contribution to the meson-glueball mixing (top). Gluon exchange to lowest order gives no contribution (bottom) for the reasons discussed in the text.

B. Glueball and meson states

In order to construct the glueball states, we have to describe the gluon cavity modes. The 4-vector potential is given by

$$A^\mu = (-A^0 \equiv \phi, \vec{A}). \quad (13)$$

Since we are working in the static cavity approximation, we will be using the Coulomb gauge

$$\vec{\nabla} \cdot \vec{A} = 0. \quad (14)$$

In this gauge, the scalar potential is given by Poisson's equation

$$-\Delta\phi = \frac{\rho}{\epsilon_0} \quad (15)$$

and thus vanishes since there are no free charges in the model considered here.

The solutions can be classified into two different classes, which are called transverse electric (TE) and transverse magnetic (TM).

Furthermore, for a spherical bag of radius R, the solutions are classified by the quantum numbers

$$l = 1, 2, \ldots \text{ orbital excitation} \quad (16)$$

$$m = -1, +1 \text{ magnetic quantum number.} \quad (17)$$

The boundary conditions generate the constraints

$$\frac{d}{dr}(r j_l(\omega r))|_{r=R} = 0 \quad (18)$$

for the TE solution and

$$j_l(\omega R) = 0 \quad (19)$$

for the TM solutions with j_l being a spherical bessel function of order l and ω is the mode energy. The transcendental equations (18) and (19) have an infinite number of solutions $\omega R = x_n$, labeled by the radial quantum number $n = 0, 1, \ldots$. The lowest modes of interest here are $l = 1$, $n = 0$, $x_{\mathrm{TE}} = 2.74$, and $x_{\mathrm{TM}} = 4.49$ [10].

The parities of the modes are $\pi = (-1)^{l+1}$ for the TE modes and $\pi = (-1)^l$ for the TM modes. The nonlinear boundary condition requires $l = 0$. This, however, is incompatible with the helicity of the gluon. Thus, we must assume that the best value for l is the lowest possible, that is $l = 1$. The lowest-lying pseudoscalar glueball with parity $J^{\pi C} = 0^{-+}$, which is the objective of our investigation, contains the lowest-lying TE mode and TM mode gluon.

Let $a^\dagger_{l\kappa mn}$ denote the particle creation operator associated with the gluon cavity state denoted by the quantum numbers l, κ, m, n, where $\kappa \in \{\mathrm{TE}, \mathrm{TM}\}$ denotes the polarization. The lowest-lying state with $\kappa = \mathrm{TE}$ is given by $l = 1$, $n = 0$ and the lowest-lying state with $\kappa = \mathrm{TM}$ is given by $l = 1$, $n = 0$. Thus, the glueball state can be constructed by

$$|G\rangle = \frac{1}{\sqrt{2}}(\hat{a}^\dagger_{\mathrm{TE}\uparrow}\hat{a}^\dagger_{\mathrm{TM}\downarrow} - \hat{a}^\dagger_{\mathrm{TE}\downarrow}\hat{a}^\dagger_{\mathrm{TM}\uparrow})|0\rangle, \quad (20)$$

where $l = 1$, $n = 0$ everywhere. We impose the restriction that the state be a color singlet.

The meson states are constructed from the cavity fermion modes. To find them, we have to study the radial solutions of the free Dirac equation. They are characterized by their total angular momentum $j = 1/2, 3/2, \ldots$, a magnetic quantum number $m = -1/2, 1/2$ and another quantum number $\lambda = -1, +1$, called Dirac's quantum number.

[1]This argument was provided to us by a referee.

The wave functions are [11]

$$u(x) = -N\begin{pmatrix} i\lambda j_l(pr) \\ \Omega j_{l'}(pr)(\vec{\sigma}\cdot\hat{\vec{x}}) \end{pmatrix}\mathcal{Y}^m_{lj}(\hat{x})e^{-i\omega t} \tag{21}$$

$$v(x) = N\begin{pmatrix} i\Omega j_{l'}(pr)(\vec{\sigma}\cdot\hat{\vec{x}}) \\ \lambda j_l(pr) \end{pmatrix}\mathcal{Y}^m_{lj}(\hat{x})e^{i\omega t}, \tag{22}$$

where $l \equiv j + \frac{1}{2}\lambda$ and $l' \equiv j - \frac{1}{2}\lambda$, $\Omega \equiv \frac{p}{\omega+m}$. In the case of a massive field, p and ω are related by $\omega = \sqrt{p^2 + m^2}$, otherwise $p \equiv \omega$. Here u denotes the particle solution and v the antiparticle solution. The object $\mathcal{Y}^m_{lj}$ is a 2-spinor of total angular momentum j, projection m and orbital angular momentum l, called spinor spherical harmonics, defined by

$$\mathcal{Y}^M_{lJ}(\hat{x}) \equiv \sum_{m\mu}\left\langle lm\frac{1}{2}\mu|JM\right\rangle Y_{lm}(\hat{x})\chi_\mu, \tag{23}$$

where χ_μ is the spin wave function Inserting Eq. (21) and (22) into the boundary condition yields the constraint

$$j_{l'}(pR) = -\frac{\lambda}{\Omega}j_l(pR). \tag{24}$$

This transcendental equation has an infinite set of solutions for each combination of j, λ. The nonlinear boundary condition requires $j = \frac{1}{2}$ for the quark states. The quark states are normalized by the requirement

$$\int_V d^3x u^\dagger(x)u(x) = \int_V d^3x v^\dagger(x)v(x) = 1. \tag{25}$$

This yields for the lowest-lying state ($j = \frac{1}{2}$, $n = 0$, $\lambda = -1$) a normalization constant of

$$N^2 = \frac{1}{R^3 j_0(\tilde{x})^2}\frac{\tilde{x}(\tilde{\nu} - mR)}{2\tilde{x}(\tilde{\nu} - 1) + mR}\frac{1}{4\pi}, \tag{26}$$

where $\tilde{x} \equiv \omega R$ and $\tilde{\nu} \equiv pR$. We have checked numerically that this is the correct formula. The normalization constant Eq. (26) in the case of massive quarks for the quark mode wave function was written incorrectly, most probably a typo, in the original paper [12], but the error has been carried on thereafter by all papers that we have used. Luckily the error does not imply large effects in the calculations involving light quarks, as can be seen in Fig. 2.

The η-mesons are pseudoscalar mesons, thus have parity $J^{PC} = 0^{-+}$. Let $\hat{b}^\dagger_{j\lambda mn}$ and $\hat{d}^\dagger_{j\lambda mn}$ denote the particle creation operator and antiparticle creation operator, respectively, associated with the fermion cavity-state denoted by the quantum numbers j, λ, m, n. We are interested in the lowest-lying meson state. The lowest energy modes are associated to the quantum numbers $j = \frac{1}{2}$, $n = 0$, $\lambda = -1$. Because of intrinsic parity between particle and antiparticle states, $P = -1$ can be obtained using the lowest-lying particle state and the lowest-lying antiparticle state. Thus, a low lying meson state, μ, can be constructed by acting with the creation operators as in

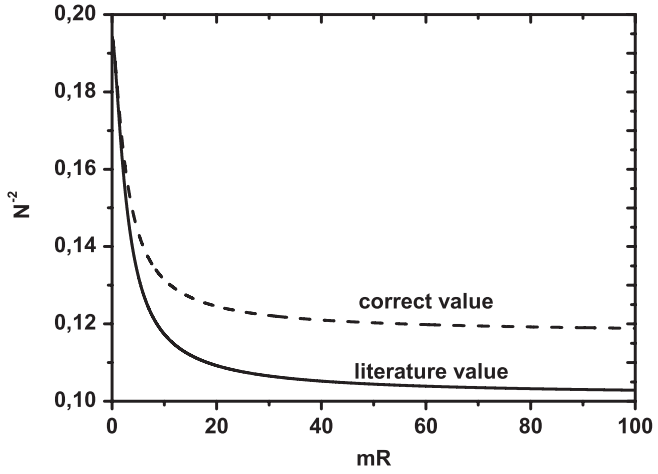

FIG. 2. Inverse square of the normalization constant of the massive bag model wavefunctions as a function of mR as appeared in [12] (lower graph) and the correct value (upper graph).

$$|\mu\rangle = \frac{1}{\sqrt{2}}(\hat{b}^\dagger_\uparrow\hat{d}^\dagger_\uparrow - \hat{b}^\dagger_\downarrow\hat{d}^\dagger_\downarrow)|0\rangle, \tag{27}$$

where $j = \frac{1}{2}$, $n = 0$, $\lambda = -1$ everywhere. We have used the notation $\uparrow, \downarrow$ for $m = \frac{1}{2}, -\frac{1}{2}$ Furthermore, we impose that it be a color singlet and the appropriate flavor composition defined by

$$\eta_8 = \frac{1}{\sqrt{6}}(u\bar{u} + d\bar{d} - 2s\bar{s}), \tag{28}$$

$$\eta_1 = \frac{1}{\sqrt{3}}(u\bar{u} + d\bar{d} + s\bar{s}). \tag{29}$$

The physical particles are defined in flavor space from the above by means of a mixing angle $\theta = 9.9 \pm 4.4^\circ$ [13–15],

$$\eta = \eta_8\cos\theta - \eta_1\sin\theta, \tag{30}$$

$$\eta' = \eta_8\sin\theta + \eta_1\cos\theta. \tag{31}$$

C. Propagators

The off-diagonal term in the energy expectation value is given by

$$E = \langle G|N\Big\{2g^2\int d^3x\bar{\psi}(x)\gamma^\mu A(x)^a_\mu t^a\int d^4x' S_F(x,x')\gamma^\nu \times A(x')^b_\nu t^b\psi(x')\Big\}|\eta(\eta')\rangle \tag{32}$$

where N denotes the normal ordering operator. This expression can be evaluated using Eq. (27) and (20) when one quantizes Eq. (12) in the manner

$$\psi(x) \rightarrow \hat{\psi}(x) = \sum_{\alpha}[u_{\alpha}(x)\hat{b}_{\alpha} + v_{\alpha}(x)\hat{d}^{\dagger}_{\alpha}] \tag{33}$$

$$\bar{\psi}(x) \rightarrow \hat{\bar{\psi}}(x) = \sum_{\alpha}[\bar{v}_{\alpha}(x)\hat{d}_{\alpha} + \bar{u}_{\alpha}(x)\hat{b}^{\dagger}_{\alpha}] \tag{34}$$

$$A(x) \rightarrow \hat{A}(x) = \sum_{\alpha}[A_{\alpha}(x)\hat{a}_{\alpha} + A^{*}_{\alpha}(x)\hat{a}^{\dagger}_{\alpha}] \tag{35}$$

with the commutation relations

$$\text{Fermion}: \{\hat{b}_{\alpha}, \hat{b}^{\dagger}_{\beta}\} = \delta_{\alpha\beta} \tag{36}$$

$$\text{Fermion}: \{\hat{d}_{\alpha}, \hat{d}^{\dagger}_{\beta}\} = \delta_{\alpha\beta} \tag{37}$$

$$\text{Gluon}: [\hat{a}_{\alpha}, \hat{a}^{\dagger}_{\beta}] = \delta_{\alpha\beta}. \tag{38}$$

Evaluating Eq. (32) with a normal-ordered operator and shifting $\hat{b}^{\dagger}$, $\hat{d}^{\dagger}$, and $\hat{a}^{\dagger}$ to the left and $\hat{b}$, $\hat{d}$, and $\hat{a}$ to the right yields

$$\text{Fermion}: \delta_{\alpha\uparrow}\delta_{\beta\uparrow} - \delta_{\alpha\downarrow}\delta_{\beta\downarrow} \tag{39}$$

$$\text{Gluon}: \delta_{\iota\text{TE}\uparrow}\delta_{\kappa\text{TM}\downarrow} - \delta_{\iota TE\downarrow}\delta_{\kappa\text{TM}\uparrow} + \delta_{\iota\text{TM}\downarrow}\delta_{\kappa\text{TE}\uparrow} - \delta_{\iota\text{TM}\uparrow}\delta_{\kappa\text{TE}\downarrow}, \tag{40}$$

where α refers to the sum index in $\bar{\psi}$ with *particle* states, β to the sum index in ψ with *antiparticle* states, ι to the sum index in the first gluon wave function A and κ to the sum index in the second gluon wave function A.

There are two possible choices for the propagator $S_F(x, x')$ in Eq. (12), namely, the cavity (confined) propagator and the free propagator. The cavity propagator is built of a complete set of cavity states in the bag model. The free propagator is the well-known Feynman propagator $S_F(x, x') = \int \frac{d^4p}{(2\pi)^4} e^{-ip\cdot(x-x')} \frac{1}{\not{p}-m+i\epsilon}$ with the Feynman prescription of closing the contour. Both propagators act as Green's functions with respect to the Dirac operator, thus formally both propagators can be used. However, since they are of a very different shape, one should expect them to generate different results. Physically, it is not clear which propagator is preferable. The cavity propagator emphasizes confinement, associated in this picture by the bag boundary conditions, while the free propagator emphasizes asymptotic freedom in the model, namely, the fact that the theory is almost free inside. We will carry out the calculation using both propagators.

(i) Cavity propagator: Since the radial solutions of the Dirac equation Eqs. (21) and (22) form a complete set, we will follow an approach by Maxwell and Vento [10] and use them to construct the cavity propagator

$$-iS_F(x, x') = \sum_{\alpha}[u_{\alpha}(x)\bar{u}_{\alpha}(x')e^{-i\omega_{\alpha}(t-t')}\theta(t-t') - v_{\alpha}(x)\bar{v}_{\alpha}(x')e^{i\omega_{\alpha}(t-t')}\theta(t'-t)] \tag{41}$$

with $\alpha = (n, \lambda, j, m)$ denoting a multiindex. Note that since the solutions represent virtual particles rather than real quark states, they are not subject to the nonlinear boundary condition and thus, values other than $j = \frac{1}{2}$ are possible.

(ii) Free propagator: The solutions generating the free propagator are not subject to the boundary conditions. Dropping the boundary conditions yields

$$\sum_{n,\lambda,J,M} \rightarrow \int_k dk \sum_{\lambda,J,M}. \tag{42}$$

Imposing the normalization condition

$$\int d^3x u^{\dagger}_k(x)u_{k'}(x) = \int d^3x v^{\dagger}_k(x)v_{k'}(x) = \delta(k-k') \tag{43}$$

yields

$$u_k(x) = \sqrt{\frac{2}{\pi}}\frac{k}{\sqrt{1+\Omega^2}} \times \begin{pmatrix} i\lambda j_l(kr) \\ \Omega j_{l'}(kr)(\vec{\sigma}\cdot\hat{\vec{x}}) \end{pmatrix} \mathcal{Y}^M_{lJ}(\hat{x})e^{-i\omega t} \tag{44}$$

$$v_k(x) = \sqrt{\frac{2}{\pi}}\frac{k}{\sqrt{1+\Omega^2}} \times \begin{pmatrix} i\Omega j_{l'}(pr)(\vec{\sigma}\cdot\hat{\vec{x}}) \\ \lambda j_l(pr) \end{pmatrix} \mathcal{Y}^M_{lJ}(\hat{x})e^{i\omega t}, \tag{45}$$

where we have used

$$\int dr r^2 j_l(kr)j_l(k'r) = \frac{\pi}{2k^2}\delta(k-k'). \tag{46}$$

This way, the calculation for the free propagator is analogous to the one shown in the appendix, with $\sum_n \rightarrow \int_k dk$ and a different normalization of ψ_{α}. This corresponds directly to Rayleigh's expansion of plane waves.

D. Time integration and recoil correction

As mentioned above, energy conservation on the vertices is not possible in the process described here since $\omega_0 \neq \omega_{\text{TE}}$ and $\omega_0 \neq \omega_{\text{TM}}$. Thus, the integrations of Eq. (12) might be formally carried out (although for specific quark masses, there arise unphysical divergences), but the physical interpretation remains unclear. It is also unclear, why the dt'-integration (corresponding to the lower vertex) has to be carried out but the dt-intergration does not, so that there will be an energy denominator only related to the

energies at the lower vertex. Apparently, there must be a (physical) inconsistency somewhere. In fact, the inconsistency is a consequence of the bag description itself. When virtual particles, that violate energy conservation, are being created, a center-of-mass motion must be expected that ultimately alters the energies of the states. This process will be taken into account here, and we will call this the recoil correction. Through the emission and absorption of the virtual fermion the states will obtain an additional center-of-mass motion energy Δ and Δ', respectively, as seen in Fig. 3, so that we are in the center-of-energy frame.

$$\omega_0 + \Delta = \omega_{\mathrm{TM}} \tag{47}$$

$$\omega_0 + \Delta' = \omega_{\mathrm{TE}}. \tag{48}$$

Only in the center-of-energy frame can the virtual fermion exchange be understood in a physically plausible way. Making this approximation, our work differs from other works in the bag model, where this issue has not been addressed.

Writing down the time dependence, which we have left out before and applying the recoil correction yields

$$\begin{aligned}\bar{u}_0(x)e^{i(\omega_0+\Delta)t}\not{A}_{\mathrm{TM}}(x)e^{-i\omega_{\mathrm{TM}}t}\int dt'[u_\alpha(x)\bar{u}_\alpha(x')e^{-i\omega_\alpha(t-t')}\\ \times\theta(t-t') - v_\alpha(x)\bar{v}_\alpha(x')e^{i\omega_\alpha(t-t')}\theta(t'-t)]\\ \times\not{A}_{\mathrm{TE}}(x')e^{-i\omega_{\mathrm{TE}}t'}v_0(x')e^{i(\omega_0+\Delta')t'},\end{aligned} \tag{49}$$

where we have left out the spatial integrations for convenience. $u_0(v_0)$ represents the lowest possible quark(antiquark) cavity state. Performing the dt' integration yields

$$\begin{aligned}\int dt' e^{i\omega_\alpha t'}\theta(t-t') &= \int_{-\infty}^{t} dt' e^{i\omega_\alpha t'} = \frac{1}{i\omega_\alpha}[e^{i\omega_\alpha t'}]_{-\infty}^{t}\\ &= \frac{e^{i\omega_\alpha t}}{i\omega_\alpha}\end{aligned} \tag{50}$$

$$\begin{aligned}\int dt' e^{-i\omega_\alpha t'}\theta(t'-t) &= \int_{t}^{\infty} dt' e^{-i\omega_\alpha t'}\\ &= -\frac{1}{i\omega_\alpha}[e^{-i\omega_\alpha t'}]_{t}^{\infty} = \frac{e^{-i\omega_\alpha t}}{i\omega_\alpha},\end{aligned} \tag{51}$$

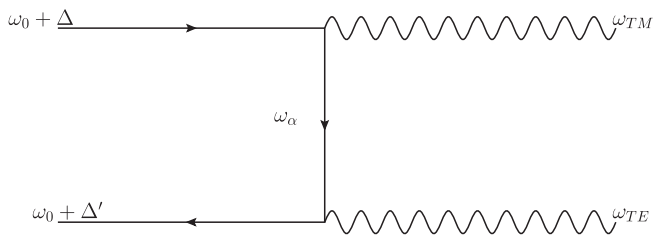

FIG. 3. Recoil correction; Energy Δ and Δ' has to be added to account for center-of-mass motion that necessarily arises through emission and absorption of the virtual particle.

where we have shifted $\omega_\alpha \to \omega_\alpha - i\epsilon$ implicitly. This gives an overall denominator of $\frac{1}{i\omega_\alpha}$ for each mode which is being propagated

III. RESULTS

After carrying out a detailed calculation, which can be found in the appendix, one obtains the mixing energy shown in Fig. 4 as a function of the quark mass times the bag radius. The mixing energy is the result of Eq. (32) using the cavity (or the free) propagator and is presented here as a function of mR and rescaled by Rg^{-2}. Here m is the quark mass, R the bag radius and g is related to the strong coupling constant in the usual way $\alpha_S = g^2/4\pi$. The mixing energy shown is per quark-pair, i.e. $q\bar{q}$.

As mentioned before we have introduced the recoil correction to make sense of the formalism and eliminate spurious contributions. In Fig. 5 we show the mixing energy obtained without the recoil correction and compare with our result. The plot of the former is dominated by an unphysical spurious singularity at $mR \approx 0.4$. Note that for physical values of the strange quark mass $m_s \sim 200$–300 and bag radii $R \sim 0.5$–1 fm one can be close to the singularity and obtain a strong mass-dependent result. On the contrary, our result is quite stable and almost constant over the interesting range. Clearly, the recoil correction is an indisposable ingredient to obtain physically meaningful results in the bag model.

The values of the pseudoscalar glueball mass change dramatically in the literature from one calculation to another. Lattice QCD in the quenched approximation leads to values around $M_G = 2500$ MeV [16–18]. Unquenched calculations should produce a lower value as happens for the scalar glueball [6,19–22]. This has been shown to be the case in an effective theory calculation of glueball

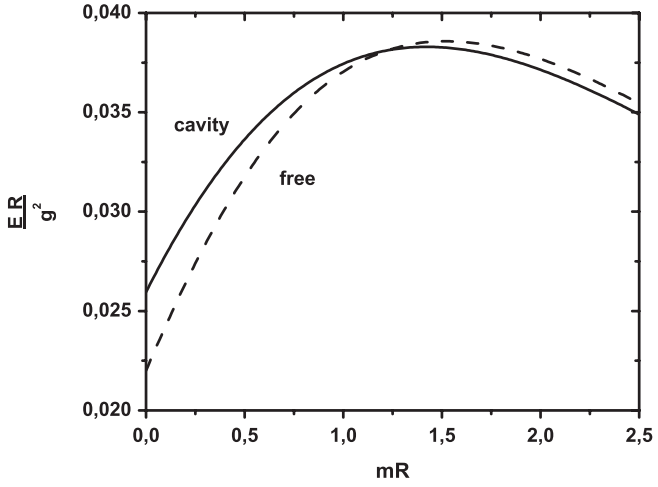

FIG. 4. Glueball-meson mixing energy per quark-antiquark pair as a function of mR for the cavity and free propagators in the η_8, η_1, G basis.

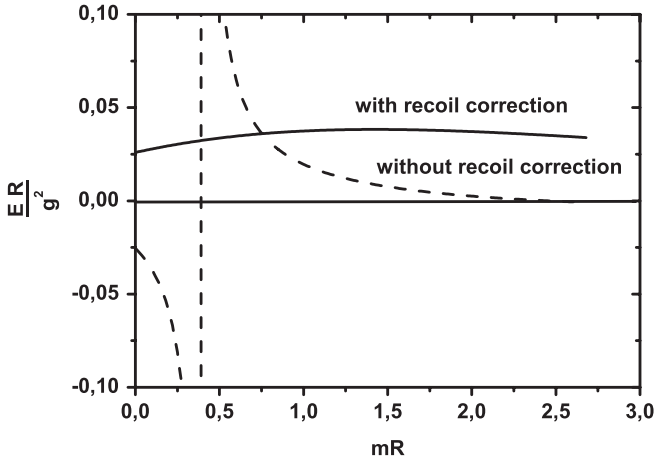

FIG. 5. Glueball-meson mixing energy per quark-antiquark pair as a function of mR for the cavity propagator with recoil correction (solid line) (as in Fig. 4) and without recoil correction (dashed line).

mixing which reproduces a large amount of data [23], where the lower pseudoscalar mass value is set at 2000 MeV. The flux-tube model [24,25] suggests a pseudoscalar glueball mass of 2570 MeV [26]. The Coulomb gauge model suggests a mass of 2220 MeV [27]. Other effective theory calculations, which fit parameters to data, lead to values down to 1400 MeV [28].

Kuti [29] suggested that a reliable glueball spectrum, which is in reasonable agreement with lattice calculations, can be obtained for $B^{1/4} = 280$ MeV and $R \approx 0.5$ fm $= 2.5\ \mathrm{GeV}^{-1}$. He gives a coupling constant $\alpha_S = 0.5$ to obtain a 0^{-+} glueball mass of about 2500 MeV in sharp contrast with the old calculation of Jaffe and Johnson [9], who chose parameters closely related to the baryon spectrum.

To calculate the mixing energy we use the results shown in Fig. 4. Note that the Y-axis of this figure is in adimensional units and also independent of the strong coupling constant. The X-axis dependence should be understood for fixed radius and varying mass. To obtain physical quantities from this figure, we have to introduce values for the radius and the strong coupling constant. This radius is not a variable but the fixed value obtained by minimizing the energy, i.e. it is determined by the value of B. To calculate the mixing energy one has to take into account the wave function of the meson states. The calculation is performed for η_8 and η_1. We do not calculate their mixing in the bag model but incorporate it phenomenologically to find the true contribution to the mixing energy of the physical mesons η and η'. To perform our mixing calculation we shall take for the mesons mass values which lead after diagonalization to the experimental ones, $\eta(550)$ and $\eta'(960)$. The mixing probability strongly depends on the glueball mass. If we choose the Kuti parameters we have in the η, η', G basis

$$\begin{pmatrix} 551 & 0 & -41 \\ 0 & 970 & 122 \\ -41 & 122 & 2500 \end{pmatrix} \qquad \eta - \eta' - G \text{ system.} \tag{52}$$

The diagonalization of this matrix produces three eigenvalues, $m_\eta = 550$ MeV, $m_{\eta'} = 960$ MeV, which coincide with the experimental determinations, $M_G = 2513$ MeV, and three eigenvectors. From the latter we obtain the mixing of $\eta - G$ to be 0.006%, and that for $\eta' - G$ to be 0.6%.

To confront the experimental situation, let us vary the mass of the glueball following the bag model prescription, i.e.

$$E = \frac{4(\omega_E + \omega_M - Z)}{3R}, \tag{53}$$

where we have eliminated B, the bag constant, through the pressure balance equation, and we have used the lowest TE and TM modes to calculate the glueball energy. Each different radius corresponds to a different B. The term Z represents the zero point energy, which we fit to have a glueball mass of 2500 MeV at a radius of 0.5 fm [29]. We omit here the perturbative contributions to the mass, which lead, for example, to the nucleon-delta mass splittings. This energy has been corrected for center-of-mass spurious motion to obtain the particle mass which we show in Fig. 6. Note that the calculation connects the Kuti and Jaffe and Johnson masses for different values of the bag radius. We show in the figure the mass of a light baryon calculated with the same zero point energy as a function of radius and see that it reaches 1100 MeV at $R = 1.0$ fm, which is the right mass value for the nucleon-delta states, if perturbative OGE corrections are not taken into account. Thus we have found a consistent approximate formula to zeroth order which ascribes the value of the glueball mass to its size and which contains all the results obtained by the different

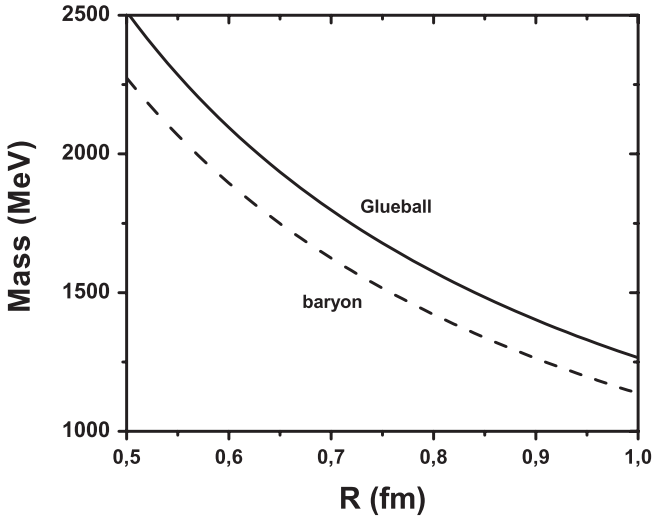

FIG. 6. Variation of glueball and baryon masses with bag radius.

calculations mentioned above. The bag radius here is a variational parameter fixed to minimize the energy. Therefore, all quantities entering the description of the systems will depend on this parameter, for example α_S, since the perturbative splittings also change with R unless we modify the coupling constant adequately. We take the R dependence of the coupling constant as $\alpha_S(R) = 2[R(\mathrm{fm})]^2$. This equation extrapolates between the two values in the literature, Kuti's (0.5) for $R = 0.5$ fm [29] and Jaffe and Johson's (2) for $R = 1$ fm [9]. Introducing all these R-dependences in Fig. 4, we calculate the mixing energies as a function of R which are shown in Fig. 7.

From the mixing energies we obtain the mixing probability by diagonalizing the mixing Hamiltonian. The Hamiltonian results, as before, in a 3×3 matrix, in the η, η', G space, whose diagonal terms are an η mass term, an η' mass term and a glueball mass term given by Eq. (53). The diagonal η and η' mass terms are chosen in a self-consistent procedure so that their values lead to the experimental determinations, $M_\eta = 550$ MeV and $M'_\eta = 960$ MeV, after diagonalization. The nondiagonal terms are the mixing terms shown in Fig. 7 (left). Thus we repeat the procedure discussed around Eq. (52) for each radius. The results are shown in Fig. 7 (right).

We note by looking at the right figure, that the proposed dynamical mechanism does not mix the η with G for reasonable values of the radius, while it can lead to large mixings of the η' with G for large bag radii. The reason for the large mixing between η' and G is that the diagonal η' and G terms become almost degenerate and that the mixing terms become large. For large bags ($R \sim 1$ fm) the self consistent procedure increases the value of the diagonal η' term to almost 1200 MeV; the R dependence drops the diagonal glueball term to slightly below 1300 MeV; and the α_S dependence increases the mixing term to 250 MeV. For the η, the situation is completely different, for large radii the diagonal term remains close to the experimental mass (570 MeV), and the mixing terms stay above -100 MeV.

It is worth mentioning, that our results deviate significantly from a prior analysis by Carlson and Hansson [30]. The difference between our work and theirs arises from our use of the recoil correction as described in Sec. II D. An additional difference is due to the use of different parameters. We show the comparison between the two curves for the mixing energy in Fig. 5. We note the spurious singularity close to the physically relevant region, which makes the results strongly dependent on the radius, if the recoil-correction is not included, while the results are very slowly dependent on the radius, if the recoil-correction is included.

The results of Fig. 7 are quite illuminating. In no case does the η mix with the glueball, even for large couplings and small glueball masses. On the contrary, the η' can mix up to 0.6% for small couplings and large glueball masses and up to 40% for small glueball masses and strong α_S. We obtain therefore a scenario strongly dependent on the glueball mass. If the glueball mass is close to the lattice value, the pseudoscalar glueball appears as an almost pure state with very distinctive features, if on the contrary the mass is small it might mix with the η' considerably but always very little with the η.

IV. CONCLUSIONS

We have performed a calculation of the mixing of the pseudoscalar glueball with the pseudoscalar mesons η and η'. Our work suggests that the mixing is small if the mass is around 2500 MeV. In the framework of the bag model,

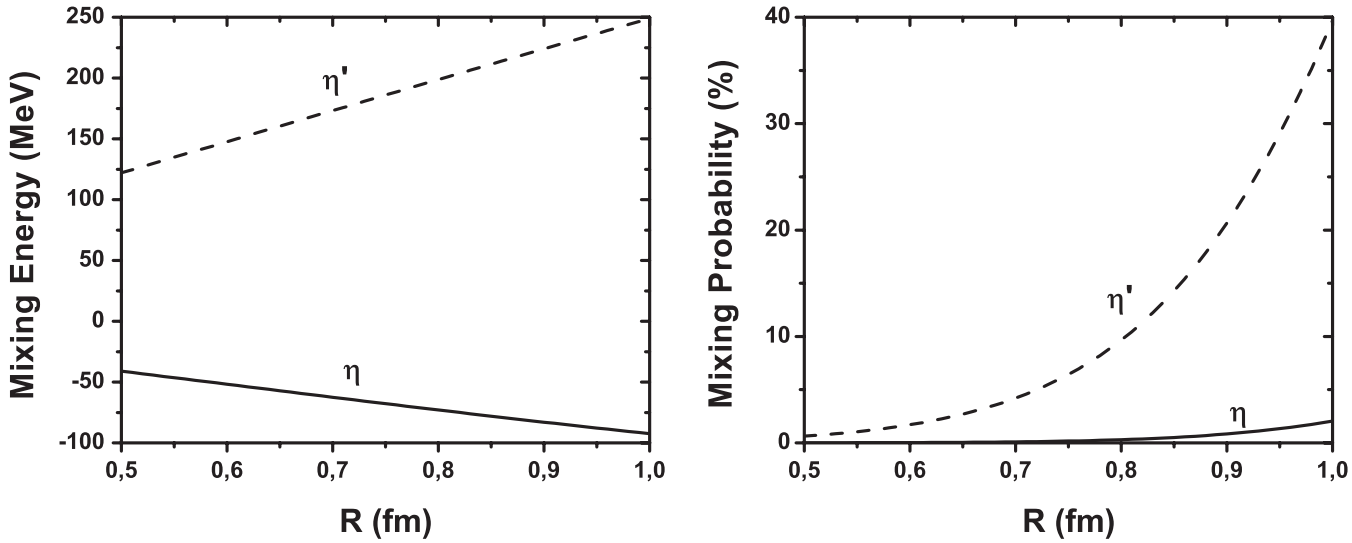

FIG. 7. η-glueball and η'-glueball mixing energies as a function of bag radius (left) and η-glueball and η'-glueball probabilities as a function of bag radius (right).

this is a new result. A previous study by Carlson and Hansson [30] suggests a much larger mixing. However, a small glueball mixing, in this glueball mass range, is as well favored by recent studies [15,28]. Accordingly, glueball mixing should not play an important role in the η-η' mass splitting. This also implies that a rather undiluted, well-defined, narrow and, therefore, long-living pseudoscalar glueball state should exist. If the mass of the glueball is closer to that of the η', around 1400 MeV, then the mixing is large and the consequences of phenomenological analyses should be reanalyzed, since the amount of mixing would determine if the glueball behaves more like mesons and baryons, i.e. large objects.

The conceptual difference between our work and other bag model calculations, like the one carried out by Carlson and Hansson [30], is the recoil correction. The recoil correction is in our opinion a necessary ingredient to carry out the calculations in a physically meaningful way by avoiding spurious singularities. The bag model in the static spherical cavity approximation fails in describing the creation and absorption of virtual particles, because in the spherical cavity, the mode energies are discrete and fixed. Thus energy conservation at the vertices is generally not possible. This subtle problem has been neglected in all previous bag model calculations so far. In our calculation it manifests as an (unphysical) singularity dominating the results for certain values of the parameters. Our way to resolve this problem is to take into account the recoil that arises in particle emission and absorption, manifesting itself necessarily in center-of-mass motion of the constituents. We add this energy to the energy of the constituents. This not only eliminates the singularity and makes way for meaningful results, but it is necessary to cancel out the time-dependence of the mixing energy. Without the recoil correction, the mixing energy is oscillating, which is also a sign of center-of-mass motion problems. All of these hints suggest that the recoil correction is correct, physical meaningful and must be applied to all bag model calculations.

At this point it is worth mentioning a technical error, which, despite its simplicity, has been in the field for many years. The normalization constant Eq. (26) in the case of massive quarks for the quark mode wave function has been used incorrectly by many authors in the past. We have shown however, that the error does not imply large effects in the calculations involving light quarks.

This work has set the standards for future calculations within the MIT bag model scheme. Any calculation dealing with the spectrum or mixings will have to follow the same procedure and approximations. In particular an interesting phenomena which we are now revisiting is the mixing of η_8 and η_1 to build the true physical η-mesons.

ACKNOWLEDGMENTS

We are grateful to V. Mathieu for interesting discussions and a careful reading of the manuscript. S. K. thanks the Departamento de Física Teórica of Valencia for the hospitality and Professor Kunz-Drolshagen for giving him the opportunity to work there. This work was supported in part by HadronPhysics2, a FP7-Integrating Activities and Infrastructure Program of the European Commission under Grant No. 227431, by the MICINN (Spain) Grant No. FPA2007-65748-C02-1 and by GVPrometeo2009/129. The diagrams have been drawn using Jaxodraw [32].

APPENDIX: DETAILS OF THE CALCULATION

Substituting Eq. (41) into Eq. (12) yields a color structure of the form

$$\bar{\psi}_i A^a \frac{\lambda^a}{2} \psi_j \bar{\psi}_j A^b \frac{\lambda^b}{2} \psi^C_k, \tag{A1}$$

where ψ^C means the charge-conjugated ψ. The gluon color singlet gives a factor of $\delta_{ab}/\sqrt{8}$ and the meson color singlet a factor of $\delta_{ii'}/\sqrt{3}$. This leads to the expression

$$\frac{\mathrm{Tr}(\lambda^a \lambda^a)}{4 \cdot \sqrt{3} \cdot \sqrt{8}}. \tag{A2}$$

Summation over a yields an additional factor of 8, which finally gives a factor of $\sqrt{\frac{2}{3}}$.

Disregarding the time dependence, we show how to calculate the spatial integrals

$$\sum_\alpha \int d^3x \bar{\psi}(x) \not{A} u_\alpha(x) \int d^3x' \bar{u}_\alpha(x') \not{A}(x') \psi(x') \tag{A3}$$

$$\sum_\alpha \int d^3x \bar{\psi}(x) \not{A} v_\alpha(x) \int d^3x' \bar{v}_\alpha(x') \not{A}(x') \psi(x') \tag{A4}$$

with the combinations

$$\begin{matrix} \bar{\psi} = \bar{u}_\uparrow,\ \psi = v_\uparrow \\ -(\bar{\psi} = \bar{u}_\downarrow,\ \psi = v_\downarrow) \end{matrix} \otimes \begin{matrix} A_1 = A_{\mathrm{TE}\uparrow},\ A_2 = A_{\mathrm{TM}\downarrow} \\ -(A_1 = A_{\mathrm{TE}\downarrow},\ A_2 = A_{\mathrm{TM}\uparrow}) \\ A_1 = A_{\mathrm{TM}\downarrow},\ A_2 = A_{\mathrm{TE}\uparrow} \\ -(A_1 = A_{\mathrm{TM}\uparrow},\ A_2 = A_{\mathrm{TE}\downarrow}) \end{matrix} \tag{A5}$$

We start with the combination $\bar{\psi} = \bar{u}_\uparrow$, $\psi = v_\uparrow$, $A = A_{\mathrm{TE}\uparrow}$, $A = A_{\mathrm{TM}\downarrow}$:

$$\sum_\alpha \underbrace{\int d^3x \bar{u}_\uparrow(x) \not{A}_{\mathrm{TE}\uparrow}(x) u_\alpha(x)}_{(1)} \underbrace{\int d^3x' \bar{u}_\alpha(x') \not{A}_{\mathrm{TM}\downarrow}(x') v_\uparrow(x')}_{(2)} \tag{A6}$$

$$(1) = \int d^3x N_0 \left[\begin{pmatrix} -ij_0(p_0 r) \\ \Omega_0 j_1(p_0 r)(\vec{\sigma} \cdot \hat{\vec{x}}) \end{pmatrix} \mathcal{Y}^{1/2}_{0^{1/2}}(\hat{x}) \right]^\dagger \gamma_0 \vec{\gamma} \cdot \frac{N_{\mathrm{TE}}}{i\omega_{\mathrm{TE}}} j_1(\omega_{\mathrm{TE}} r) \vec{Y}^1_{11}(\hat{x}) N_\alpha \begin{pmatrix} i\lambda j_l(p_\alpha r) \\ \Omega_\alpha j_{l'}(p_\alpha r)(\vec{\sigma} \cdot \hat{\vec{x}}) \end{pmatrix} \mathcal{Y}^M_{lJ}(\hat{x}) \tag{A7}$$

Note that

$$\vec{\sigma}\cdot\hat{\vec{x}}\mathcal{Y}^M_{lJ}(\hat{x}) = -\mathcal{Y}^M_{l'J} \tag{A8}$$

with $l' = l - \lambda = J - \frac{1}{2}\lambda$ and, furthermore,

$$\gamma_0\vec{\gamma} = \begin{pmatrix}1 & 0\\ 0 & -1\end{pmatrix}\begin{pmatrix}0 & \vec{\sigma}\\ -\vec{\sigma} & 0\end{pmatrix} = \begin{pmatrix}0 & \vec{\sigma}\\ \vec{\sigma} & 0\end{pmatrix} \tag{A9}$$

which yields

$$\begin{aligned}(1) = N_0N_\alpha\frac{N_{\mathrm{TE}}}{i\omega_{\mathrm{TE}}}&\\ \times\int d^3x(ij_0(p_0r)\mathcal{Y}^{1/2\dagger}_{0^{1/2}}, -\Omega_0 j_1(p_0r)\mathcal{Y}^{1/2\dagger}_{1^{1/2}})&\\ \times\begin{pmatrix}0 & \vec{\sigma}\cdot\vec{Y}^1_{11}\\ \vec{\sigma}\cdot\vec{Y}^1_{11} & 0\end{pmatrix}&\\ \cdot\begin{pmatrix}i\lambda j_l(p_\alpha r)\mathcal{Y}^M_{lJ}\\ -\Omega_\alpha j_{l'}(p_\alpha r)\mathcal{Y}^M_{l'J}\end{pmatrix}j_1(\omega_{\mathrm{TE}}r)\Omega_\alpha j_{l'}(p_\alpha r)&\end{aligned} \tag{A10}$$

$$\begin{aligned}= N_0N_\alpha\frac{N_{\mathrm{TE}}}{i\omega_{\mathrm{TE}}}\int d^3x[-ij_0(p_0r)\Omega_\alpha j_{l'}(p_\alpha r)\mathcal{Y}^{1/2\dagger}_{0^{1/2}}\vec{\sigma}&\\ \cdot\vec{Y}^1_{11}\mathcal{Y}^M_{l'J} - \Omega_0 j_1(p_0r)i\lambda j_l(p_\alpha r)\mathcal{Y}^{1/2\dagger}_{1^{1/2}}\vec{\sigma}\cdot\vec{Y}^1_{11}\mathcal{Y}^M_{lJ}]&\\ \times j_1(\omega_{\mathrm{TE}}r).&\end{aligned} \tag{A11}$$

Consider the relation [31]

$$\begin{aligned}\mathcal{Y}^{M_1\dagger}_{L_1J_1}\vec{\sigma}\mathcal{Y}^{M_2}_{L_2J_2} = (-1)^{J_2+L_1+M_1}&\\ \times\sqrt{\frac{3(2J_1+1)(2J_2+1)(2L_1+1)(2L_2+1)}{2\pi}}&\\ \times\sum_{JL}(-1)^J\langle L_10L_20|L0\rangle\begin{Bmatrix}L_1 & J_1 & \frac{1}{2}\\ L_2 & J_2 & \frac{1}{2}\\ L & J & 1\end{Bmatrix}&\\ \times\langle J_1 - M_1J_2M_2|JM\rangle\vec{\mathcal{Y}}^L_{JM}&\end{aligned} \tag{A12}$$

and, furthermore, the orthogonality

$$\int\vec{\mathcal{Y}}^{M'*}_{L'J'}(\hat{x})\cdot\vec{\mathcal{Y}}^M_{LJ}(\hat{x})d\Omega = \delta_{J'J}\delta_{L'L}\delta_{M'M} \tag{A13}$$

and also

$$\vec{\mathcal{Y}}^{M*}_{LJ}(\hat{x}) = (-1)^{J+L+M+1}\vec{\mathcal{Y}}^{-M}_{LJ}(\hat{x}). \tag{A14}$$

These relations allow us to express

$$\int\mathcal{Y}^{1/2\dagger}_{0^{1/2}}\vec{\sigma}\cdot\vec{Y}^1_{11}\mathcal{Y}^M_{l'J}d\Omega = \int[\mathcal{Y}^{1/2\dagger}_{0^{1/2}}\vec{\sigma}\mathcal{Y}^M_{l'J}]\cdot\vec{Y}^{-1*}_{11}d\Omega. \tag{A15}$$

It is now obvious that only the term $J = 1$, $L = 1$ of the sum in Eq. (A12) survives. Furthermore, $\langle L_10L_20|L0\rangle = \langle 00l'0|10\rangle$ tells us that $l' = 1$, which allows only the modes $J = \frac{1}{2}$, $\lambda = -1$ and $J = \frac{3}{2}$, $\lambda = 1$. The factor $\langle J_1 - M_1J_2M_2|JM\rangle = \langle\frac{1}{2} - \frac{1}{2}JM|1\ -1\rangle$ requires $M = -\frac{1}{2}$. The expression

$$\int[\mathcal{Y}^{1/2\dagger}_{1^{1/2}}\vec{\sigma}\mathcal{Y}^M_{lJ}]\cdot Y^{-1*}_{11}d\Omega \tag{A16}$$

requires $l = 0, 2$, which allows the modes $J = \frac{1}{2}$, $\lambda = -1$, $J = \frac{3}{2}$, $\lambda = 1$, and $J = \frac{5}{2}$, $\lambda = -1$. The last mode, however, is prohibited by the second Clebsch-Gordan coefficient in Eq. (A12). Thus, the $d\Omega_x$-integral constraints the values for J, λ, M in Eq. (A6), while the sum goes over all possible n.

(1) of Eq. (A6) takes the form

$$\begin{aligned}&J = 1/2,\\ &\lambda = -1\text{: } j_1(\omega_{\mathrm{TE}}r)[-ij_0(\omega_0r)\Omega_\alpha j_1(\omega_\alpha r)\\ &\quad\times\alpha(0, 1/2, 1/2\parallel 1, 1/2, -1/2\parallel 1, 1)\\ &\quad+\Omega_0 j_1(\omega_0r)j_0(\omega_\alpha r)\\ &\quad\times\alpha(1, 1/2, 1/2\parallel 0, 1/2, -1/2\parallel 1, 1)]\end{aligned} \tag{A17}$$

$$\begin{aligned}&J = 3/2,\\ &\lambda = 1\text{: } j_1(\omega_{\mathrm{TE}}r)[-ij_0(\omega_0r)j_1(\omega_\alpha r)\\ &\quad\times\Omega_\alpha\alpha(0, 1/2, 1/2\parallel 1, 3/2, -1/2\parallel 1, 1)\\ &\quad-i\Omega_0 j_1(\omega_0r)j_2(\omega_\alpha r)\\ &\quad\times\alpha(1, 1/2, 1/2\parallel 2, 3/2, -1/2\parallel 1, 1)]\end{aligned} \tag{A18}$$

where we left out the expression $N_0N_\alpha\frac{N_{\mathrm{TE}}}{i\omega_{\mathrm{TE}}}\int drr^2$ for convenience. We introduce

$$\begin{aligned}&\alpha(L_1, J_1, M_1\parallel L_2, J_2, M_2\parallel L, J)\\ &\quad\equiv(-1)^{J+J_2+L_1+M_1}\\ &\qquad\times\sqrt{\frac{3(2J_1+1)(2J_2+1)(2L_1+1)(2L_2+1)}{2\pi}}\\ &\qquad\times\langle L_10L_20|L0\rangle\begin{Bmatrix}L_1 & J_1 & \frac{1}{2}\\ L_2 & J_2 & \frac{1}{2}\\ L & J & 1\end{Bmatrix}\langle J_1 - M_1J_2M_2|JM\rangle\end{aligned} \tag{A19}$$

A list of expressions for α can be found in Table I

(2) of Eq. (A6) becomes:

$$\begin{aligned}&J = 1/2,\\ &\lambda = -1\text{: }\sqrt{\tfrac{2}{3}}j_0(\omega_{\mathrm{TM}}r')[ij_0(\omega_\alpha r')j_0(\omega_0r')\alpha(0, 1/2, -1/2\\ &\quad\parallel 0, 1/2, 1/2\parallel 0, 1) - \Omega_\alpha j_1(\omega_\alpha r')i\Omega_0 j_1(\omega r')\\ &\quad\times\alpha(1, 1/2, -1/2\parallel 1, 1/2, 1/2\parallel 0, 1)]\\ &\quad-\sqrt{\tfrac{1}{3}}j_2(\omega_{\mathrm{TM}}r')[-\Omega_\alpha j_1(\omega_\alpha r')i\Omega_0 j_1(\omega_0r')\\ &\quad\times\alpha(1, 1/2, -1/2\parallel 1, 1/2, 1/2\parallel 2, 1)]\end{aligned} \tag{A20}$$

TABLE I. α coefficients.

L_1	J_1	M_1	L_2	J_2	M_2	L	J	α
1	1/2	1/2	0	1/2	−1/2	1	1	$-\sqrt{\frac{1}{3\pi}}$
0	1/2	1/2	1	3/2	−1/2	1	1	$\sqrt{\frac{1}{24\pi}}$
1	1/2	1/2	2	3/2	−1/2	1	1	$-\sqrt{\frac{1}{24\pi}}$
0	1/2	−1/2	0	1/2	1/2	0	1	$-\sqrt{\frac{1}{2\pi}}$
1	3/2	−1/2	1	1/2	1/2	2	1	$-\frac{\sqrt{2}}{12\sqrt{\pi}}$
1	1/2	−1/2	1	1/2	1/2	2	1	$\frac{2}{3\sqrt{\pi}}$
1	3/2	−1/2	1	1/2	1/2	0	1	$\frac{1}{3\sqrt{\pi}}$
0	1/2	1/2	2	3/2	−1/2	2	1	$\frac{\sqrt{2}}{4\sqrt{\pi}}$
1	1/2	−1/2	1	1/2	1/2	0	1	$\frac{\sqrt{2}}{6\sqrt{\pi}}$

$J = 3/2,$

$$\begin{aligned}\lambda = 1\sqrt{\tfrac{2}{3}} j_0(\omega_{\mathrm{TM}} r')[&-\Omega_\alpha j_1(\omega_\alpha r') i\Omega_0 j_1(\omega_0 r') \\ &\times \alpha(1, 3/2, -1/2 \parallel 1, 1/2, 1/2 \parallel 0, 1)] \\ &- \sqrt{\tfrac{1}{3}} j_2(\omega_{\mathrm{TM}} r')[-i j_2(\omega_\alpha r') j_0(\omega_0 r') \alpha(2, 3/2, \\ &- 1/2 \parallel 0, 1/2, 1/2 \parallel 2, 1) - \Omega_\alpha j_1(\omega_\alpha r') i\Omega_0 j_1(\omega_0 r') \\ &\times \alpha(1, 3/2, -1/2 \parallel 1, 1/2, 1/2 \parallel 2, 1)] \end{aligned} \tag{A21}$$

where we left out the expression $-N_0 N_\alpha \frac{N_{\mathrm{TM}}}{\omega_{\mathrm{TM}}} \int dr' r'^2$. The additional minus sign comes from the fact that $\vec{Y}_{01}^{M*} = -\vec{Y}_{01}^{-M}$ and $\vec{Y}_{21}^{M*} = -\vec{Y}_{21}^{-M}$, while $\vec{Y}_{11}^{M*} = \vec{Y}_{11}^{-M}$.

In order for the combinations in (A5) to give a nonzero contribution, the spins have to be aligned as $\bar{u}_\uparrow A_\uparrow A_\downarrow v_\uparrow$ or $\bar{u}_\downarrow A_\downarrow A_\uparrow v_\downarrow$. This corresponds to $M_1 \to -M_1$, $M_2 \to -M_2$ in α (A19). Because of

$$\frac{\alpha(L_1, J_1, M_1 \parallel L_2, J_2, M_2 \parallel L, J)}{\alpha(L_1, J_1, -M_1 \parallel L_2, J_2, -M_2 \parallel L, J)} = (-1)^{J_1 + J_2 - J + 1} \quad \text{where } M_1, M_2 \in \{-1/2, 1/2\} \tag{A22}$$

the signs from the two integrals cancel. Thus, the combinations with inverse magnetic quantum number give the same contribution.

Next, we consider the expression

$$\bar{u}_0 \vec{\gamma} \cdot \vec{A}_{\mathrm{TE}} u_\alpha \bar{u}_\alpha \vec{\gamma} \cdot \vec{A}_{\mathrm{TM}} v_0 \tag{A23}$$

$$= u_0^\dagger \gamma^0 \vec{\gamma} \cdot \vec{A}_{\mathrm{TE}} u_\alpha u_\alpha^\dagger \gamma^0 \vec{\gamma} \cdot \vec{A}_{\mathrm{TM}} i\gamma^2 u_0^* \tag{A24}$$

where we inserted the definition for the charge-conjugated particle state. Since this expression has the form of a c-number, we transpose it by Hermitian conjugation and complex conjugation. Hermitian conjugation gives

$$u_0^{*\dagger}(-\gamma^2)(-i)(-\vec{\gamma} \cdot \vec{A}_{\mathrm{TM}}^*)\gamma^0 u_\alpha u_\alpha^\dagger (-\vec{\gamma} \cdot \vec{A}_{\mathrm{TE}}^*)\gamma^0 u_0. \tag{A25}$$

Complex conjugation gives

$$\begin{aligned} &u_0^\dagger \gamma^2 i(\vec{\gamma} \cdot \vec{A}_{\mathrm{TM}} - 2[\vec{A}_{\mathrm{TM}}]_y \gamma^2) \\ &\quad \times \gamma^0 u_\alpha^* u_\alpha^{*\dagger} (\vec{\gamma} \cdot \vec{A}_{\mathrm{TE}} - 2[\vec{A}_{\mathrm{TE}}]_y \gamma^2)\gamma^0 u_0^* \end{aligned} \tag{A26}$$

$$\begin{aligned} &= -u_0^\dagger i(\vec{\gamma} \cdot \vec{A}_{\mathrm{TM}})\gamma^2 \gamma^0 u_\alpha^* u_\alpha^{*\dagger} \gamma^2 \gamma^2 (\vec{\gamma} \cdot \vec{A}_{\mathrm{TE}} - 2[\vec{A}_{\mathrm{TE}}]_y \gamma^2) \\ &\quad \times \gamma^0 u_0^* \end{aligned} \tag{A27}$$

$$= -u_0^\dagger \gamma^0 (\vec{\gamma} \cdot \vec{A}_{\mathrm{TM}}) i\gamma^2 u_\alpha^* u_\alpha^{*\dagger} \gamma^2 (\vec{\gamma} \cdot \vec{A}_{\mathrm{TE}}) \gamma^2 \gamma^0 u_0^* \tag{A28}$$

$$= -\bar{u}_0 (\vec{\gamma} \cdot \vec{A}_{\mathrm{TM}}) v_\alpha u_\alpha^{*\dagger} \gamma^2 \gamma^0 (\vec{\gamma} \cdot \vec{A}_{\mathrm{TE}}) \gamma^2 u_0^* \tag{A29}$$

$$= \bar{u}_0 (\vec{\gamma} \cdot \vec{A}_{\mathrm{TM}}) v_\alpha u_\alpha^{*\dagger} \gamma^2 \gamma^0 i(\vec{\gamma} \cdot \vec{A}_{\mathrm{TE}}) \gamma^2 u_0^* \tag{A30}$$

$$= \bar{u}_0 (\vec{\gamma} \cdot \vec{A}_{\mathrm{TM}}) v_\alpha \bar{v}_\alpha (\vec{\gamma} \cdot \vec{A}_{\mathrm{TE}}) v_0. \tag{A31}$$

For the last step, we have used $\bar{v} = (i\gamma^2 u^*)^\dagger \gamma^0 = i u^{*\dagger} \gamma^2 \gamma^0$.

Taking into account the definition of the cavity propagator (41) as well as the time integration with the recoil correction, one finds that the combinations with TE $\leftrightarrow$ TM give the same contribution. Thus, there is an overall symmetry factor of 4 for the different combinations of wave functions.

$\bar{u}_0 \not{A}_{\mathrm{TE}} S_F \not{A}_{\mathrm{TM}} v_0$, particle propagation:

$J = 1/2,$

$$\begin{aligned} \lambda = -1\text{: } &\left\{-i\Omega_\alpha \sqrt{\frac{1}{3\pi}} j_0(\omega_0 r) j_1(\omega_\alpha r) j_1(\omega_{\mathrm{TE}} r) - i\Omega_0 \sqrt{\frac{1}{3\pi}} j_1(\omega_0 r) j_0(\omega_\alpha r) j_1(\omega_{\mathrm{TE}} r)\right\} \\ &\times \left[\sqrt{\frac{2}{3}}\left\{-i\sqrt{\frac{1}{2\pi}} j_0(\omega_0 r') j_0(\omega_\alpha r') j_0(\omega_{\mathrm{TM}} r') - i\frac{\sqrt{2}}{6\sqrt{\pi}} \Omega_\alpha \Omega_0 j_1(\omega_0 r') j_1(\omega_\alpha r') j_0(\omega_{\mathrm{TM}} r')\right\}\right. \\ &\left. - \sqrt{\frac{1}{3}}\left\{-i\frac{2}{3\sqrt{\pi}} \Omega_\alpha \Omega_0 j_1(\omega_0 r') j_1(\omega_\alpha r') j_2(\omega_{\mathrm{TM}} r')\right\}\right] \end{aligned} \tag{A32}$$

$$
\begin{aligned}
&J = 3/2,\\
&\lambda = 1\text{:}\ \left\{-i\Omega_\alpha\sqrt{\frac{1}{24\pi}}j_0(\omega_0 r)j_1(\omega_\alpha r)j_1(\omega_{\mathrm{TE}} r) + i\Omega_0\sqrt{\frac{1}{24\pi}}j_1(\omega_0 r)j_2(\omega_\alpha r)j_1(\omega_{\mathrm{TE}} r)\right\}\\
&\quad\times\left[\sqrt{\frac{2}{3}}\left\{-i\frac{1}{3\sqrt{\pi}}\Omega_\alpha\Omega_0 j_1(\omega_0 r')j_1(\omega_\alpha r')j_0(\omega_{\mathrm{TM}} r')\right\} - \sqrt{\frac{1}{3}}\left\{+i\frac{\sqrt{2}}{4\sqrt{\pi}}j_0(\omega_0 r')j_2(\omega_\alpha r')j_2(\omega_{\mathrm{TM}} r')\right.\right.\\
&\quad\left.\left. + i\frac{\sqrt{2}}{12\sqrt{\pi}}\Omega_\alpha\Omega_0 j_1(\omega_0 r')j_1(\omega_\alpha r')j_2(\omega_{\mathrm{TM}} r')\right\}\right]
\end{aligned}
\tag{A33}
$$

$\bar{u}_0 \not{A}_{\mathrm{TE}} S_F \not{A}_{\mathrm{TM}} v_0$, antiparticle propagation:

$$
\begin{aligned}
&J = 1/2,\\
&\lambda = 1\text{:}\ \left\{-i\sqrt{\frac{1}{3\pi}}j_0(\omega_0 r)j_1(\omega_\alpha r)j_1(\omega_{\mathrm{TE}} r) + i\sqrt{\frac{1}{3\pi}}\Omega_0\Omega_\alpha j_1(\omega_0 r)j_0(\omega_\alpha r)j_1(\omega_{\mathrm{TE}} r)\right\}\\
&\quad\times\left[\sqrt{\frac{2}{3}}\left\{i\sqrt{\frac{1}{2\pi}}\Omega_\alpha j_0(\omega_0 r')j_0(\omega_\alpha r')j_0(\omega_{\mathrm{TM}} r') - i\frac{1}{6}\sqrt{\frac{2}{\pi}}\Omega_0 j_1(\omega_0 r')j_1(\omega_\alpha r')j_0(\omega_{\mathrm{TM}} r')\right\}\right.\\
&\quad\left. - \sqrt{\frac{1}{3}}\left\{-i\frac{2}{3\sqrt{\pi}}\Omega_0 j_1(\omega_0 r')j_1(\omega_\alpha r')j_2(\omega_{\mathrm{TM}} r')\right\}\right]
\end{aligned}
\tag{A34}
$$

$$
\begin{aligned}
&J = 3/2,\\
&\lambda = -1\text{:}\ \left\{i\sqrt{\frac{1}{24\pi}}j_0(\omega_0 r)j_1(\omega_\alpha r)j_1(\omega_{\mathrm{TE}} r) + i\sqrt{\frac{1}{24\pi}}\Omega_0\Omega_\alpha j_1(\omega_0 r)j_2(\omega_\alpha r)j_1(\omega_{\mathrm{TE}} r)\right\}\\
&\quad\times\left[\sqrt{\frac{2}{3}}\left\{i\frac{1}{3\sqrt{\pi}}\Omega_0 j_1(\omega_0 r')j_1(\omega_\alpha r')j_0(\omega_{\mathrm{TM}} r')\right\} - \sqrt{\frac{1}{3}}\left\{-i\Omega_\alpha\frac{\sqrt{2}}{4\sqrt{\pi}}j_0(\omega_0 r')j_2(\omega_\alpha r')j_2(\omega_{\mathrm{TM}} r')\right.\right.\\
&\quad\left.\left. - i\Omega_0\frac{\sqrt{2}}{12\sqrt{\pi}}j_1(\omega_0 r')j_1(\omega_\alpha r')j_2(\omega_{\mathrm{TM}} r')\right\}\right]
\end{aligned}
\tag{A35}
$$

For convenience, we have left out the expression $-i\sum_n N_0^2 N_\alpha^2 \frac{N_{\mathrm{TE}} N_{\mathrm{TM}}}{i\omega_{\mathrm{TE}}\omega_{\mathrm{TM}}} \int dr r^2 \int dr' r'^2$. Also, one has a factor of $2g^2 \cdot 4 \cdot \frac{1}{2} \cdot \sqrt{\frac{2}{3}}$, which arises from Eq. (12), the symmetry in the combinations, the wave function symmetrization and the color matrix trace, respectively. For the cavity propagator, it is important to note the J, λ quantum numbers, because the modes ω_α depend on these quantum numbers as well as on the n quantum number, which is summed over.

[1] H. Fritzsch, M. Gell-Mann, and H. Leutwyler, Phys. Lett. **47B**, 365 (1973).
[2] D. J. Gross and F. Wilczek, Phys. Rev. Lett. **30**, 1343 (1973).
[3] H. D. Politzer, Phys. Rev. Lett. **30**, 1346 (1973).
[4] K. G. Wilson, Phys. Rev. D **10**, 2445 (1974).
[5] V. Mathieu, N. Kochelev, and V. Vento, Int. J. Mod. Phys. E **18**, 1 (2009).
[6] V. Crede and C. A. Meyer, Prog. Part. Nucl. Phys. **63**, 74 (2009).
[7] D. L. Scharre *et al.*, Phys. Lett. **97B**, 329 (1980).
[8] H. Fritzsch and P. Minkowski, Nuovo Cimento Soc. Ital. Fis. A **30**, 393 (1975).
[9] R. L. Jaffe and K. Johnson, Phys. Lett. **60B**, 201 (1976).
[10] O. V. Maxwell and V. Vento, Nucl. Phys. A **A407**, 366 (1983).
[11] A. Messiah, *Mécanique Quantique* (Dunod, Paris, 1962), Vol. 2.
[12] T. A. DeGrand, R. L. Jaffe, K. Johnson, and J. E. Kiskis, Phys. Rev. D **12**, 2060 (1975).
[13] F. Ambrosino *et al.* (KLOE Collaboration), Phys. Lett. B **648**, 267 (2007).
[14] C. E. Thomas, J. High Energy Phys. 10 (2007) 026.
[15] R. Escribano, Eur. Phys. J. C **65**, 467 (2010).
[16] C. J. Morningstar and M. J. Peardon, Phys. Rev. D **60**, 034509 (1999).
[17] H. B. Meyer and M. J. Teper, Phys. Lett. B **605**, 344 (2005); H. B. Meyer, arXiv:hep-lat/0508002.

[18] Y. Chen *et al.*, Phys. Rev. D **73**, 014516 (2006).
[19] J. Sexton, A. Vaccarino, and D. Weingarten, Phys. Rev. Lett. **75**, 4563 (1995).
[20] A. Hart and M. Teper (UKQCD Collaboration), Phys. Rev. D **65**, 034502 (2002).
[21] C. McNeile, Proc. Sci., LATTICE2007 (2007) 019.
[22] A. Hart *et al.* (UKQCD Collaboration), Phys. Rev. D **74**, 114504 (2006).
[23] V. Mathieu and V. Vento, Phys. Rev. D **81**, 034004 (2010).
[24] N. Isgur and J. E. Paton, Phys. Lett. **124B**, 247 (1983).
[25] N. Isgur and J. E. Paton, Phys. Rev. D **31**, 2910 (1985).
[26] M. Iwasaki, S. I. Nawa, T. Sanada, and F. Takagi, Phys. Rev. D **68**, 074007 (2003).
[27] A. P. Szczepaniak and E. S. Swanson, Phys. Lett. B **577**, 61 (2003).
[28] H. Y. Cheng, H. n. Li, and K. F. Liu, Phys. Rev. D **79**, 014024 (2009).
[29] J. Kuti, Nucl. Phys. B, Proc. Suppl. **73**, 72 (1999).
[30] C. E. Carlson and T. H. Hansson, Nucl. Phys. **B199**, 441 (1982).
[31] D. A. Varshalovich, A. N. Moskalev, and V. K. Khersonskii, *Quantum Theory of Angular Momentum* (World Scientific, Singapore, 1988).
[32] D. Binosi and L. Theussl, Comput. Phys. Commun. **161**, 76 (2004).